Supplemental Material to "Universal Scaling Theory of the Boundary Geometric Tensor in Disordered Metals"

Miklós Antal Werner and Gergely Zaránd
MTA-BME Exotic Quantum Phases "Momentum" Research Group, Department of Theoretical Physics, Budapest University of Technology and Economics, 1111 Budapest, Budafoki út 8, Hungary

Arne Brataas
Center for Quantum Spintronics, Department of Physics, Norwegian University of Science and Technology, NO-7491 Trondheim, Norway

Felix von Oppen
Dahlem Center for Complex Quantum Systems and Fachbereich Physik, Freie Universität Berlin, 14195 Berlin, Germany
(Dated: February 20, 2019)

S 1. EXPLICIT FORMULAS FOR THE BOUNDARY GEOMETRIC TENSOR

In this section we derive explicit expressions for the quantum geometric tensor (QGT)[S1], used in our analysis. The Hamiltonian, Eq. (2) of the main text, is supplemented by twisted boundary conditions. In a finite system, this boundary condition appears through the hopping terms at the boundary: there electron operators outside the boundary ($\mathbf{r}'$) are replaced by phase shifted operators inside the boundary, $\mathbf{r} = \mathbf{r}' - \mathbf{n}L$, as

$$c_{\mathbf{r}'} = e^{i\mathbf{n}\cdot\boldsymbol{\phi}} c_{\mathbf{r}} \ , \tag{S1}$$

with $\mathbf{n} = (n_x, n_y, n_z)$ appropriately chosen integers and $\boldsymbol{\phi} = (\phi_x, \phi_y, \phi_z)$ the boundary twists. We can restore the periodic boundary conditions by performing the gauge transformation,

$$\tilde{c}_{\mathbf{r}} = e^{-\frac{i}{L}\mathbf{r}\cdot\boldsymbol{\phi}} c_{\mathbf{r}} \ , \tag{S2}$$

In terms of these, the Hamiltonian becomes

$$\hat{H} = \sum_{\mathbf{r}} V(\mathbf{r}) \tilde{c}^{\dagger}_{\mathbf{r}} \tilde{c}_{\mathbf{r}} - \sum_{\langle \mathbf{r},\mathbf{r}' \rangle} \left(t_{\mathbf{r}\mathbf{r}'} \ e^{\frac{i}{L}(\mathbf{r}-\mathbf{r}')\cdot\boldsymbol{\phi}} \ \tilde{c}^{\dagger}_{\mathbf{r}} \tilde{c}_{\mathbf{r}'} + h.c. \right) \ . \tag{S3}$$

To express the QGT, we need the derivatives

$$\frac{\partial \hat{H}}{\partial \phi_k} = - \sum_{\langle \mathbf{r},\mathbf{r}' \rangle} \left(\frac{i}{L} (r_k - r'_k) t_{\mathbf{r}\mathbf{r}'} \ e^{\frac{i}{L}(\mathbf{r}-\mathbf{r}')\cdot\boldsymbol{\phi}} \ \tilde{c}^{\dagger}_{\mathbf{r}} \tilde{c}_{\mathbf{r}'} + h.c. \right) \ . \tag{S4}$$

Expanding then $\hat{H}(\boldsymbol{\phi} + d\boldsymbol{\phi}) = \hat{H}(\boldsymbol{\phi}) + d\boldsymbol{\phi} \cdot \frac{\partial \hat{H}}{\partial \boldsymbol{\phi}} + \dots$ and performing first order perturbation theory in $d\boldsymbol{\phi}$ we obtain

$$Q_{ij}(\alpha) = \sum_{\beta \neq \alpha} \frac{\langle \alpha | \, \partial \hat{H}/\partial \phi_i \, | \beta \rangle \, \langle \beta | \, \partial \hat{H}/\partial \phi_j \, | \alpha \rangle}{(E_\alpha - E_\beta)^2} \ . \tag{S5}$$

S 2. THE QUANTUM GEOMETRIC TENSOR AND THE THOULESS NUMBER

The Thouless number[S2], defined as the disorder averaged absolute curvature of the single particle energies at energy E, divided by the mean level spacing Δ at E, is a commonly used indicator in the field of Anderson transitions,

$$\mathcal{C}_T = \frac{\pi}{\Delta} \left\langle \left| \frac{\partial^2 E_\alpha}{\partial \phi_x^2} \right| \right\rangle_{E_\alpha = E} \tag{S6}$$

Similar to the parameter $g_{\rm typ}$ (see (6) in the main text), it is a function of energy, system size, disorder strength, and magnetic field. As argued in Ref. S2, and numerically demonstrated in Ref. S3, the Thouless number (S6) measures the dimensionless DC conductance of a finite system.

Fig. S1 shows the connection between the Thouless number and the parameter $g_{\rm typ} \sim \mathrm{tr}\, Q$. We observe an approximately linear connection between the two parameters; however, a significant difference appears in the dependence of $\mathcal{C}_T$ on $g_{\rm typ}$ in the presence, or absence of a strong enough external magnetic field. Nevertheless, the one-to-one connection between $g_{\rm typ}$ and $\mathcal{C}_T$ in the universal limits implies analogous one parameter scaling properties for both $\mathcal{C}_T$ and $g_{\rm typ}$. Using $g_{\rm typ}$ instead of the Thouless number is therefore a legitimate choice.

S 3. FINITE SIZE SCALING OF THE QGT IN A HOMOGENEOUS MAGNETIC FIELD

As stated in the main text, one cannot observe the orthogonal-unitary crossover in homogeneous magnetic fields, because there is at least one flux quantum pierced through a system on a torus. As shown in Fig. S2, the extracted RG trajectories fall on two distinct lines in the $\{g_{\rm typ}, h_{\rm typ}\}$ plane for $B = 0$ and $B \neq 0$. Even in the smallest magnetic field we could simulate ($B = \Phi_0/196$ in the units of flux/cell, and $L = 14$), the data points fall on the same line corresponding to the $B \neq 0$ universality class, and we cannot observe any trace of the unitary-orthogonal crossover in homogeneous fields. The positions of $B \neq 0$ trajectories and critical points in Fig. S2 coincide with the ones in Fig. 1 of the main text computed in a random field. This agreement strongly supports that models with homogeneous and strong random fields fall in the same universality class.

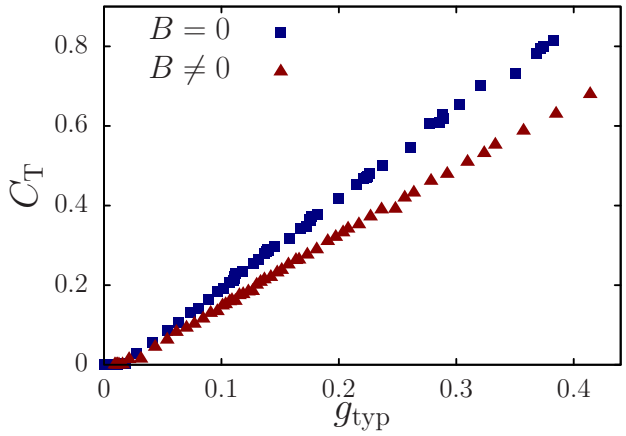

FIG. S1. The Thouless number $\mathcal{C}_T$ as a function of the parameter $g_{\rm typ}$: the precise relation between these two parameters depends on the universality class. In case of a homogeneous or strong random magnetic field, one finds the same $\mathcal{C}_T(g_{\rm typ})$ function, which is clearly different from the one obtained for $B = 0$.

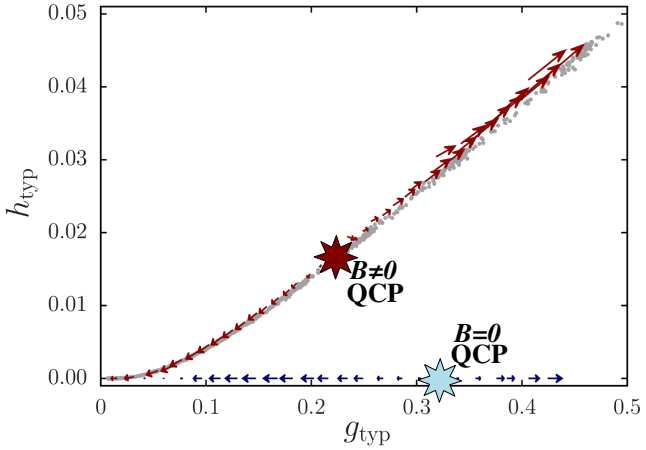

FIG. S2. Finite size scaling of the parameters $g_{\rm typ}$ and $h_{\rm typ}$ in homogeneous (red arrows) and zero (blue arrows) magnetic fields. The renormalization group trajectories fall on distinct one parameter curves in the two cases. The quantum critical points of the $B = 0$ (orthogonal) and $B \neq 0$ (unitary) universality classes are denoted by light blue and dark red stars, respectively. The flow in homogeneous field is calculated using a field strength of $B = \Phi_0/9$, while the system size is increased from $L = 9$ to $L = 12$. The gray dots show the data in the smallest simulated homogeneous field, $B = \Phi_0/196$, with $L = 14$.

The inset of Fig. S2 shows the one parameter β-functions ($\beta(g_{\rm typ}) = \partial \ln g_{\rm typ}/\partial \ln L$) in the two universality classes. In addition we show the naively calculated β-functions in weak random magnetic fields, obtained by calculating numerically the derivative $\partial \ln g_{\rm typ}/\partial \ln L$ by increasing the system size from $L = 8$ to $L = 14$. We find a "motion" of these naive curves from the $B = 0$ to the $B \neq 0$ universal β functions upon increasing the size of the random field. This continuous crossover demonstrates the failure of the one parameter scaling theory in weak random fields: there is necessarily a second relevant scaling variable at the orthogonal critical point that describes the crossover.

S 4. DETAILS OF FITTING THE CRITICAL POINTS AND EXPONENTS

To extract the critical parameters of the fixed points in the RG flow of Fig. 1. we rewrite Eq. (6) into a vectorial form and then linearize the equation around the fixed points to get

$$\frac{\partial}{\partial \ln L}\begin{pmatrix} g_{\rm typ} \\ h_{typ} \end{pmatrix} = \begin{pmatrix} M_{gg} & M_{gh} \\ M_{hg} & M_{hh} \end{pmatrix}\left[\begin{pmatrix} g_{\rm typ} \\ h_{typ} \end{pmatrix} - \begin{pmatrix} g^*_{\rm typ} \\ h^*_{typ} \end{pmatrix}\right] = \begin{pmatrix} M_{gg} & M_{gh} \\ M_{hg} & M_{hh} \end{pmatrix}\begin{pmatrix} g_{\rm typ} \\ h_{typ} \end{pmatrix} - \begin{pmatrix} b_g \\ b_h \end{pmatrix} . \tag{S7}$$

Here $g^*_{\rm typ}$ and $h^*_{\rm typ}$ denote the coordinates of the corresponding fixed point, while the matrix $\underline{\underline{M}}$ drives the linearized flow. In (S7) we introduced the vector $\begin{pmatrix} b_g \\ b_h \end{pmatrix} = \underline{\underline{M}} \begin{pmatrix} g^*_{\rm typ} \\ h^*_{typ} \end{pmatrix}$ to transform (S7) into a form where the dependence on the parameters $\underline{\underline{M}}$, b_g, and b_h is linear. We can then use the machinery of multivariate linear regression to extract $\underline{\underline{M}}$ and $\underline{b}$[S4]. The coordinates of the fixed point are then expressed as $\begin{pmatrix} g^*_{\rm typ} \\ h^*_{\rm typ} \end{pmatrix} = \underline{\underline{M}}^{-1}\underline{b}$, while the critical exponents y_1 and y_2 corresponding to the fixed point are the eigenvalues of $\underline{\underline{M}}$. At the orthogonal ($B = 0$) fixed point, one can further exploit the fact that in the absence of the magnetic field the parameter $h_{\rm typ}$ vanishes, and thereby reduce the number of fitting parameters from 6 to 4.

S 5. THE CRITICAL DISTRIBUTION OF $g(\alpha)$

We have determined numerically the critical distribution of the trace of the geometric tensor, $g(\alpha) = \mathrm{tr}\{Q_\alpha\}$, both at the orthogonal and at the unitary critical points. The observed $p(g)$ functions, shown in Fig. S3, are similar at the two critical points, but exhibit important differences, too (see panels (a) and (b) of Fig. S3). At both critical points, $p(g)$ displays power-law tails $\sim g^{-\eta}$ at large g. However, while at the unitary critical point we observe an exponent $\eta \approx 2.5$, at the orthogonal critical point $\eta \approx 2$ seems to emerge. Both exponents are consistent with the expression, $\eta = \beta/2 + 3/2$, with $\beta = 1$ and $\beta = 2$ the usual parameters classifying the orthogonal and unitary universality classes, respectively. The exponent η is clearly different from the exponent $\tilde{\eta} = 2 + \beta$ characterizing the distribution of the Thouless curvatures, $c_\alpha \equiv \pi\,|\partial^2_\phi E_\alpha|/\Delta$, defined as the dimensionless level curvature, with Δ referring to the typical level spacing (see red data points in Fig. S3).

The observed exponent $\eta = \beta/2 + 3/2$ follows from the expression Eq. (S5) under the assumption that the sum is dominated by a single term with an anomalously small level separation, $s \equiv |E_\alpha - E_{\beta=\alpha+1}| \ll \Delta$. By relying on the result that small level separations obey Wigner-Dyson statics even at the critical point[S5], $p(s) \propto s^\beta$, we arrive immediately at the prediction, $p(g) \propto g^{-(\beta/2+3/2)}$ for large g. Similar arguments imply a fall-off $p(c) \propto c^{-(\beta+2)}$ for the distribution of the level dependent Thouless curvature, c_α[S6–S8].

S 6. DETAILED ISOTROPY ANALYSIS AT THE $B \neq 0$ (UNITARY) FIXED POINT

As stated in the main text, the unitary ($B \neq 0$) critical point has a surprising isotropy: at the critical point the direction of a homogeneous magnetic field appears to be irrelevant. In addition, the joint distribution of the generalized parameters h_k seems to have full rotational symmetry (O(3)) at first sight (see Fig. 2 in the main text). Here we show in more details that, according to our data, the full O(3) symmetry is slightly broken and lowered to the discrete octahedral symmetry, interpreted as an effect of the cubic shape of our system.

The QGT, as defined in Eq. (1), follows the usual transformation laws of tensors under rotations: i.e. if one

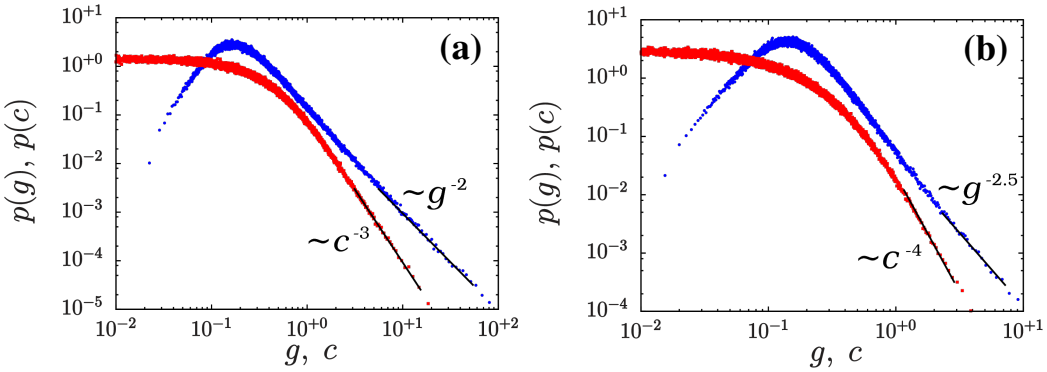

FIG. S3. **(a)-(b)** Critical distributions of the trace of the geometric tensor, $g(\alpha) = \mathrm{tr}\{Q_\alpha\}$, and the dimensionless level curvature $c_\alpha = \pi\,|\partial^2 E_\alpha/\partial\phi^2|/\Delta$ at the orthogonal ($B = 0$) and unitary ($B \neq 0$) critical points, respectively. Blue symbols represent the distribution $p(g)$, while red symbols represent $p(c)$. The observed exponents are consistent with the predictions of random-matrix theory.

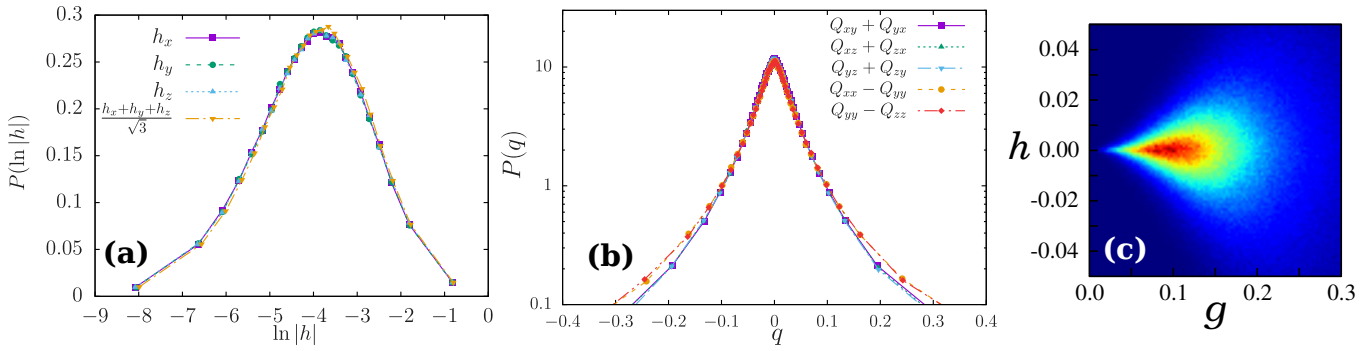

FIG. S4. (a) Probability density function of $\ln|h_i|$ and $\ln(|h_x+h_y+h_z|/\sqrt{3})$. In the latter case the distribution slightly distorts, that is an evidence for the breaking of the full rotational symmetry. (b) Probability density functions of $Q_{xy}+Q_{yx}$, $Q_{xz}+Q_{zx}$, $Q_{yz}+Q_{zy}$, $Q_{xx}-Q_{yy}$, and $Q_{yy}-Q_{zz}$. The distribution slightly differs for the latter two case, that is again an evidence for breaking of the full rotational symmetry. (c) Joint critical distribution of $h=h_z$ and $g=\mathrm{tr}\{Q\}$.

transforms the twist phases $\underline{\phi}=(\phi_x,\phi_y,\phi_z)$ with an orthogonal transformation $\underline{\phi}\to\underline{\underline{O}}\,\underline{\phi}$, then the QGT transforms as

$$\underline{\underline{Q}}\to\underline{\underline{O}}\,\underline{\underline{Q}}\,\underline{\underline{O}}^T\,. \tag{S8}$$

At the critical points the QGT is a random variable, with a probability density function $P\left(\underline{\underline{Q}}\right)$. The transformation $\underline{\underline{O}}$ is a symmetry of the distribution, if

$$P\left(\underline{\underline{Q}}\right)\equiv P\left(\underline{\underline{O}}\,\underline{\underline{Q}}\,\underline{\underline{O}}^T\right) \tag{S9}$$

for every $\underline{\underline{Q}}$.

The parameters h_k introduced in Eq. (11) parametrize the antisymmetric part of the tensor. As a result, these parameters follow the usual transformation laws of (axial-)vectors under orthogonal transformations,

$$\underline{h}'=\det(\underline{\underline{O}})\,\underline{\underline{O}}\,\underline{h}\,. \tag{S10}$$

Consequently, if the distribution of $\underline{\underline{Q}}$ had full $O(3)$ symmetry, the joint distribution of parameters h_k would be spherically symmetric. One consequence of such a high symmetry on the marginal distributions would be the relations

$$P(h_i)\stackrel{?}{=}P(h_j)\stackrel{?}{=}P\left((h_i+h_j+h_k)/\sqrt{3}\right)\,, \tag{S11}$$

with $i\neq j\neq k$. To test this symmetry, we first determine the typical magnitudes in the critical point, $(h_k)_{\mathrm{typ}}=0.01683(13)$, and $\left((h_i+h_j+h_k)/\sqrt{3}\right)_{\mathrm{typ}}=0.01769(11)$. This slight change is also directly visible in the probability density function. The distribution of $\ln|h|$ is shown in Fig. S4, and only a slight shift is visible in the case of $(h_i+h_j+h_k)/\sqrt{3}$; however, the distortion of the distribution is hardly visible.

The breaking of the rotational symmetry is stronger in the symmetric part of the QGT. If the tensor was O(3) symmetric, the following combinations would be equivalent,

$$P\left(Q_{xy}+Q_{yx}\right),\ P\left(Q_{yz}+Q_{zy}\right),\ P\left(Q_{zx}+Q_{xz}\right),\ P\left(Q_{xx}-Q_{yy}\right),\ \text{and}\ P\left(Q_{yy}-Q_{zz}\right)\,. \tag{S12}$$

As shown in panel (b) of Fig. S4, for $Q_{xx}-Q_{yy}$ and $Q_{yy}-Q_{zz}$ the distributions are significantly distorted. The separation of the diagonal and off-diagonal combinations can be explained as an effect of the lowering of the full O(3) symmetry to the discrete octahedral (O_h) symmetry group.

We believe that in an infinite system the critical point should have full isotropy, i.e. the microscopic direction of the lattice gets irrelevant. In a finite system, however, the critical state extends over the whole system, and it is therefore unavoidably affected by the boundaries.

It is important to note that the isotropy does not imply the independence of various parameters. As an example, the joint critical distribution of $h=h_z$ and $g=\mathrm{tr}\{Q\}$ is shown in Fig. S4c. It is apparent from the sepecific form of

the distribution, that there is a strong correlation between the magnitudes of g and h, i.e. the two parameters are not independent.

[S1] M. Kolodrubetz, D. Sels, P. Mehta, and A. Polkovnikov, Physics Reports **697,** 1 (2017).
[S2] J. T. Edwards and D. J. Thouless, J. Phys. C **5,** 807 (1972).
[S3] D. Braun, E. Hofstetter, G. Montambaux, and A. MacKinnon, Phys. Rev. B **55**, 7557 (1997).
[S4] R. Christensen, Advanced Linear Modeling (Springer-Verlag, New York, 2001), Second Edition.
[S5] B. I. Shklovskii, B. Shapiro, B. R. Sears, P. Lambrianides, and H. B. Shore, Phys. Rev. B, **47**, 11487 (1993).
[S6] F. von Oppen, Phys. Rev. Lett. **73**, 798 (1994).
[S7] F. von Oppen, Phys. Rev. E **51**, 2647 (1995).
[S8] C. M. Canali, Chaitali Basu, W. Stephan, and V. E. Kravtsov, Phys. Rev. B **54,** 1431 (1996).